A Simple Model for Lateral Torsional Buckling Resistance of Steel I-Beams Under Fire Conditions – Comparison with Experimental Results

Piloto, P. A. G.[1]; Vila Real, P. M. M.[2]; Franssen, J.-M.[3]

[1]*Applied Mechanics Department, Polytechnic Institute of Bragança, Ap. 134, 5301-857 Bragança, Portugal*
[2]*Department of Civil Engineering, University of Aveiro, 3810 Aveiro, Portugal*
[3]*University of Liege, 1, Chemin des Chevreuils, 4000 Liège, Belgium*

Abstract

When a beam is bent about its axis of greatest flexural rigidity it may twist before it reaches its strength limit state. This flexural stability limit state is most commonly referred to as *lateral torsional buckling* of a beam. The twisting of the beam occurs when the compression flange becomes unstable as a result of its being subjected to flexural induced axial stresses. Lateral torsional buckling is of importance when the compression flange is laterally unsupported as is often the case in continuous beams, cantilever beams, frame beams and frame columns.

The aim of this work is to develop a simple model, i. e., an analytical method to be used by designers for the calculation of the resistance moment of steel I-beams failing by lateral torsional buckling when submitted to the fire.

A particular attention has been paid to the possibility to use the same model as the one proposed in Eurocode 3 – Part 1-1, simply modifying material properties according to the temperature. This is the procedure currently proposed in Eurocode 3 – Part 1-2, although its accuracy has never been demonstrated and can indeed be questioned. Due to the fact that higher temperatures usually develop at the end of the flanges than in the rest of the section, the decrease of the bending stiffness in case of fire is faster around the weak axis than around the strong axis of the section. The method has been developed from a set of experimental results performed at elevated temperatures.

As it is known any analytical, numerical or theoretical model is much more likely to be accepted if it is backed and supported by a set of experimental tests. Comparison of the simple model has been made with laboratory test results obtained in the framework of this work. A set of experimental full-scale tests were performed on IPE100 profiles at elevated temperature for several length specimens from 0.5 meter to 6.5 meters of buckling length. Residual stresses, geometrical imperfections and material strength were measured for each tested element.

The load was applied after the heating of the beams. The beams were electric heated by means of ceramic mat elements. Automatic control on different heating devices was presented in order to ensure a uniform temperature distribution along the length of the elements. The temperature field has been measured with thermocouples welded on the beams.

A Set of experimental results are presented, relating the critical load with the mid span movement of the beam cross section, when submitted to a constant moment distribution and to a uniform distributed load, due to the ceramic mat and the insulation material weight.

Keywords: Lateral buckling; Experimental validation; Simple model; Fire action.

[2] Corresponding author. E.mail: pvreal@civil.ua.pt; Tel: 351-234370094; Fax: 351-234370094

1- INTRODUCTION

The lateral torsional buckling resistance of steel beams is well known at room temperature, but in accidental situation of fire, the guides for designers are undifferentiated regarding the temperature and they are not supported by experimental results. In this work it is presented a full scale test at elevated temperatures for determining the buckling behavior of simple supported steel IPE beams.

Some numerical simulations of the same tested beams are being made and should be presented soon for model verification and steel structures design. The behavior will be material and geometrical non linear.

The tests presented were done as a result of a Portuguese R&D national project PRAXIS/P/ECM/14176/1998 “lateral buckling of steel beams under fire conditions” and intend to be a contribution on the knowledge of structures in fire.

The Experimental set-up is presented in the figure 1 and is constituted by two parts. One for the thermal domain and another for the structural purpose.

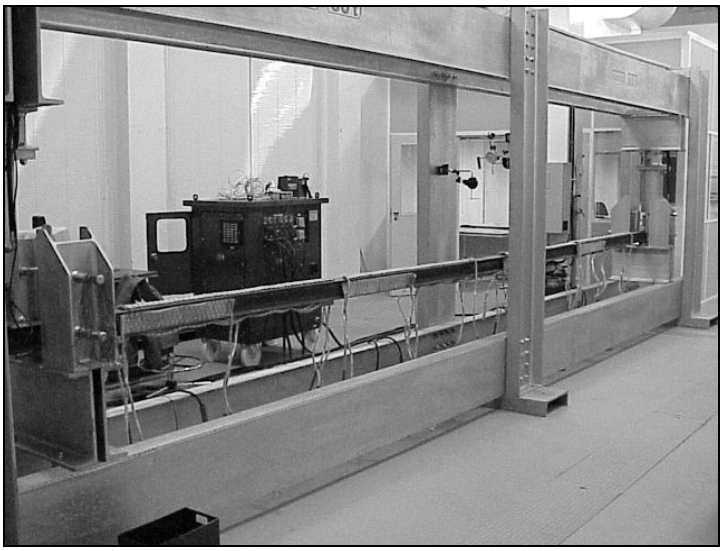

Fig.1 – Experimental set-up for lateral torsional buckling behavior of structures.

The heating system must have the necessary components for thermal energy generation. The temperature variation for rise and fall should be controlled, the heating elements should deliver the necessary power, provide the thermal insulation for best efficiency and a set of accessories for mounting the complete system are required.

The structural system should be stable with adjustable supports and load points. The structure used is modular and multi- functional. The Electro Hydraulic system is capable of delivery 60 [ton] force in each point load, and has the possibility of programming the rise and rate of force respect to time. The control unit as the capability of store the pick force value.

Regarding the phenomenon of lateral torsional buckling in [1], this document give the possibility of determining the design buckling resistance moment of a laterally unrestrained beam with a class1 or 2 cross section, in case of fire as it is presented in the equation (1).

$$M_{b,fi,t,Rd} = \frac{\chi_{LT,fi}}{1.2} w_{pl,y} k_{y,\theta,com} f_y \frac{1}{\gamma_{M,fi}} \quad (1)$$

In this reference and provided that the non dimensional slenderness $\overline{\lambda}_{LT,\theta,com}$ for the maximum temperature in the compression flange $\theta_{a,com}$ reached at time “t” does not exceed 0.4 no allowance need be made for this situation. When non dimensional slenderness exceed that value

the design moment should be calculated by expression (1). In this expression $\chi_{LT,fi}$ represents the reduction coefficient in fire situation, $w_{pl,y}$ is the plastic modulus of the beam cross section, $k_{y,\theta,com}$ is the reduction factor of the yield strength that accounts for temperature variation.

The aim of this work is to present an alternative expression to calculate the design moment resistance and validate the results with full scale tests.

2- LATERAL TORSIONAL BUCKLING OF STEEL I BEAMS

When a beam is bent about is axis of greatest flexural rigidity it may twist before it reaches its strength limit state. This stability limit state is most commonly referred to as *lateral torsional buckling* of a beam. The twisting of the beam occurs when the compression flange becomes unstable as a result of its being subjected to flexural induced axial stresses. Lateral buckling is of importance when the compression flange is laterally unsupported as is often the case in continuous beams, cantilever beams, frame beams and frame columns.

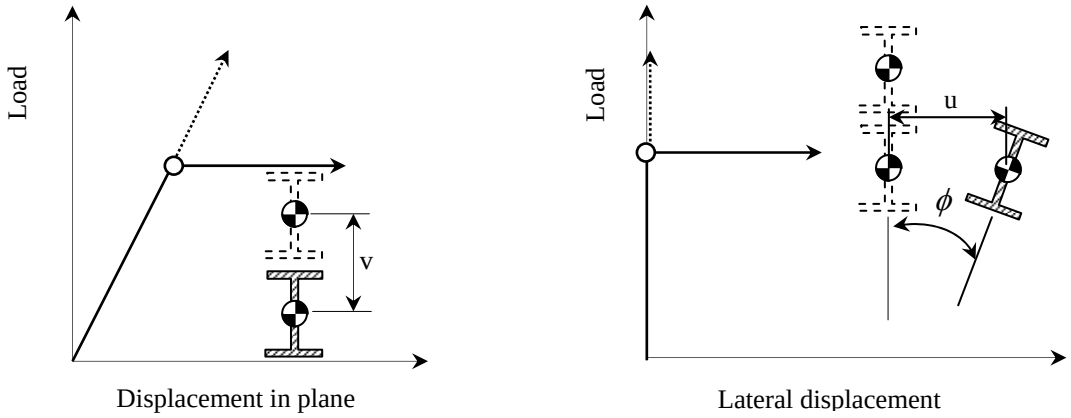

Fig.2- Graphics representation of the cross section movement.

The lateral torsional buckling of beams (Figure 2) involves lateral displacement u out of the plane of bending and twist rotations ϕ. In this case, the twist rotations makes the applied moments to have components acting out of the original plane of bending, while the lateral rotations du/dz cause the applied moments to have torque components about the axis of twist through the shear center.

Methods for designing against lateral torsional buckling are essential of two types. For the first type, buckling is avoided, and the member in plane capacity is fully utilized. One way of achieving this is to use beam cross sections not susceptible to buckle, such as hollow sections. A second way of avoiding buckling is to increase bracing, either by reducing its spacing, or else by increasing its effectiveness. For the second type a reduced capacity is determined which accounts for the effects of flexural torsional buckling.[2]

The case presented in this paper is about a simple supported beam with two forks at the supports, uniform distributed load (due to the weight of the heating system and insulation) and a moment at the ends of the beam, as shown in the figure 3.

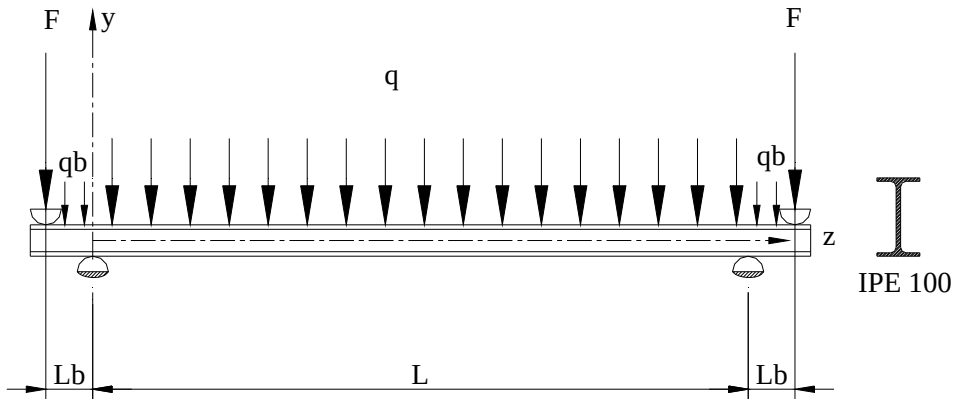

Fig. 3 – Case study. Simply supported beam with two forks separated by the buckling length L[m].

The bending moment distribution with transverse load varies along the beam and so the differential equations have some variable coefficients and are difficult to solve.

2.1- Critical elastic moment.

For the case when the load acts at the shear center, and for double symmetric beams, the elastic critical moment varies with the type of load.

When a beam is bent, the section may deforms in its plane, move laterally u and twist ϕ into an adjacent position as shown in figure 4. The minor axis moment $M_x\phi$ causes the lateral movement, and the torque $M_x u'$ is responsible for the twist rotations.

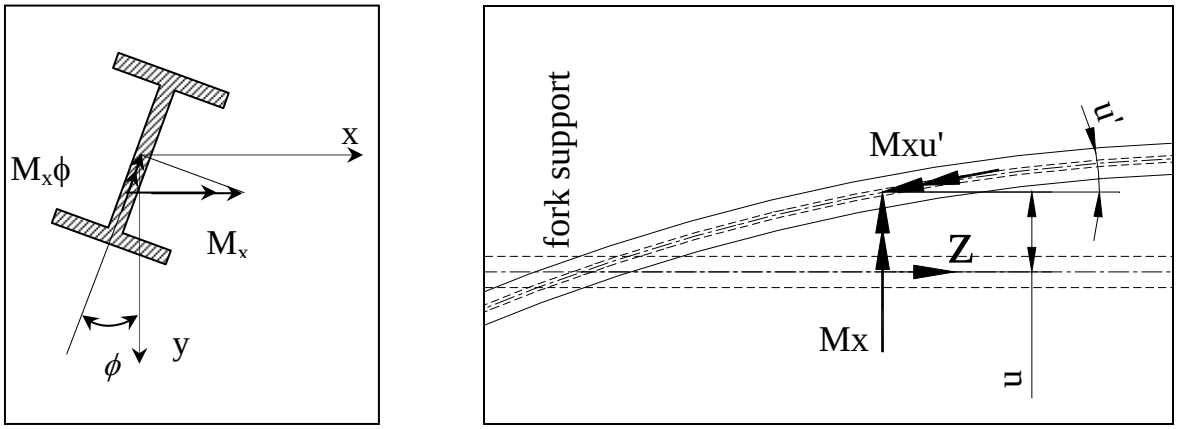

Fig.4 – Out of plane moment. Interdependence of "u" and "ϕ"

Then for this position to be in equilibrium the differential equations are:

$$\left(EI_y u''\right)'' + \left(M_x \phi\right)'' = 0$$

$$\left(EI_w \phi''\right)'' - \left(GJ\phi'\right)' + \left(M_x u''\right) = 0 \qquad (2)$$

The first equation expresses the equality between the flexural resistance $\left(EI_y u''\right)''$ and the lateral bending action $-\left(M_x \phi\right)''$ of the bending moment caused by this rotation. The second equation expresses the equality between the sum of internal warping and uniform torsion resistance $\left[\left(EI_w \phi''\right)'' - \left(GJ\phi'\right)'\right]$ and the distributed torque generated by warping and twisting of the beam, during buckling.

It can be verified by substitution that these equations are satisfied by the buckled shapes:

$$\frac{u}{\delta} = \frac{\phi}{\theta} = sin\left(\frac{\pi z}{L}\right) \tag{3}$$

or still by the simply formula

$$\frac{u}{\delta} = \frac{\phi}{\theta} = \frac{z}{L} - \frac{z^2}{L^2} \tag{4}$$

where δ and θ represent the values of u and ϕ at mid span and z the coordinate along the beam axis, provided the value of the applied moments M.

For the present case the beam should verify the equilibrium equations 2 and also the energy equation 5.

$$\frac{1}{2}\int_0^L \left(EI_y u''^2 + EI_w \phi''^2 + GJ\phi'^2\right)dz + \frac{1}{2}\int_0^L 2M_x \phi\, u'' dz + \frac{1}{2}\int_0^L q(y_q - y_0)\phi^2\, dz = 0 \tag{5}$$

which represents the equality at buckling between the flexural, warping and torsional strain energy stored and the work done by the bending moment M_x and the distributed load q, acting at a distance y_q from the shear center y_0.

The condition of neutral equilibrium at bifurcation buckling follows from the principle of conservation of energy. As the structure under a fixed set of loads buckles from an unbuckled position in a quasi static manner to an adjacent buckled position which is one of equilibrium, the increase in the strain energy $1/2\,\delta^2 U$ stored in the structure is matched by an equal decrease in the potential energy $-1/2\,\delta^2 V$ of the loads. Thus the equation 5 may be expressed as.

$$\frac{1}{2}\left(\delta^2 U + \delta^2 V\right) = 0 \tag{6}$$

Substituting the equation (4) and all the derivatives into equation 5 and taking into account the moment distribution along the buckling length, it can be verified that the critical load is a function of the material properties, the geometric characteristics of the beam cross section and also a function of the distributed load. That result can be compared to the critical elastic moment for the constant moment load case, using the buckling factor α_M , as shown in equation 7.

$$M_{cr} = \alpha_M \times \frac{\pi^2 EI_z}{L^2} \times \sqrt{\frac{I_w}{I_z} + L^2 \times \frac{GI_t}{\pi^2 EI_z}} \tag{7}$$

This coefficient is not constant and depends on the buckling length of the tested beam, as can be seen in the figure 5.

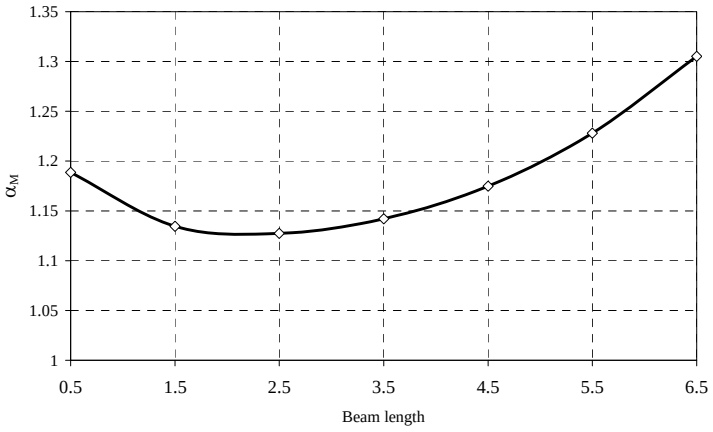

Fig.5- Coefficient for critical elastic moment.

3- MATERIAL PROPERTIES UNDER FIRE CONDITIONS

When submitted to fire conditions, the material properties of steel I beams will change due to the fact of a metallurgic transformation. In the figure 6 it can be shown the difference between the dimensions of the microstructure of the material at room temperature and after being submitted to fire condition. The specimen was heated to 600 [ºC] at 800 [ºC/h], and after that, the beam was naturally cooled to the room temperature.

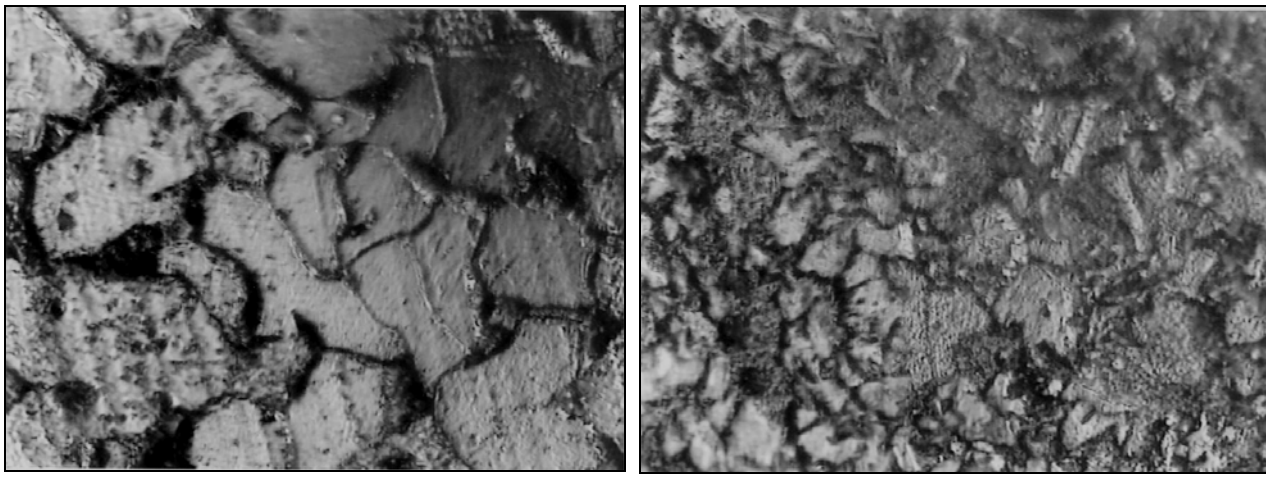

Fig. 6- Micro structure of the steel grade in study at normal conditions and after heated to 600 [ºC] and cooled naturally to normal conditions. (Amplified 500X)

This difference will be much more amplified during a fire situation and it will present a drastic change in thermal and mechanical properties.

Structure-insensitive properties are those which are not influenced significantly by changes in microstructure or macrostructure. It is recognized that many of the physical properties of a material, e.g. elastic modulus, bulk density, specific heat, and coefficient of thermal expansion, do not vary other than by small amounts from specimen to specimen of a given material, even if the different specimens have been subjected to very different working and/or heat treatment processes. This insensitive is present despite the fact that these processes may have produced quite substantial microstructural and macrostructural modifications. On the other hand most of the mechanical properties are very dependent on these modifications. Thus, for instance, the yield strength, ductility and fracture strength are seen to be structure-sensitive.

3.1- Mechanical properties.

The first model to represent the behavior of steel materials in fire situation used simple methods of calculation. Thus the extrapolation was the only way to represent the difference at elevated temperatures regarding the values at room temperature.

The stress – strain relationship used at 20 [ºC] and all the other necessary parameters were studied and established several values of deformation 0.2%, 0.5% and 2% to represent or define the yield of the material. The elastic and perfectly plastic models are still in used, but has it is presented in [3], the results will be much more close to reality if a bi linear relation with an increased hardening effect of the material is used.

The results of Rubert and Schaumann [4] were transposed to the Eurocodes, and they established a model in which the material creep would be considered in a implicit way. Their non stationary tests were done over a IPE80 and IPE 120 beams with a heat rate between 2.67 and 32 [ºC/min] and they permit to established an analytical elliptic expression to represent the behavior of the material before yielding.

For temperatures below 400 [ºC] the stress strain relationship specified in Eurocodes may be extended by hardening option, provided that the proportions of the cross section are not such that local buckling is liable to prevent attainment of the increased strain and that the member is adequately restrain to prevent buckling, as can be seen in the figure 7.[1]

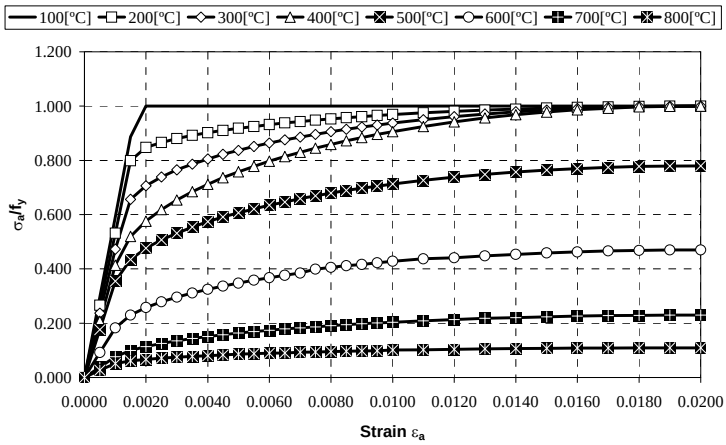

Fig. 7- Variation of stress- strain relationship with temperature for grade S355 steel. Hardening effect not included.

3.1.1.- Coefficient of thermal elongation

Even when the structural element is not loaded, the steel material has the capability of deformation by the action of the temperature. The temperature elevation impose an increase of the beam length due to the material elongation. By definition this coefficient is obtained by mathematical differentiation of the thermal deformation ε_{th}, relative to normal temperature, as it is indicated in the equation 8.

$$\frac{d\varepsilon_{th}}{d\theta} = \alpha \tag{8}$$

where α represents the material coefficient of thermal elongation and θ the material temperature. This coefficient is consider independent of the steel grade. Results presented in [5,6,7,8,9] show that the approximation of equation 9 represents approximately the material behavior.

$$\begin{gathered}
\varepsilon_{th} = -2.416\times10^{-4} + 1.2\times10^{-5}\times\theta_a + 0.4\times10^{-8}\times\theta_a{}^2; \;\; 20 < \theta_a \le 750[^{o}\mathrm{C}] \\
\varepsilon_{th} = 11.0\times10^{-3}; \;\; 750 < \theta_a \le 860[^{o}\mathrm{C}] \\
\varepsilon_{th} = -6.2\times10^{-3} + 2.0\times10^{-5}\times\theta_a; \;\; 860 < \theta_a \le 1200[^{o}\mathrm{C}]
\end{gathered} \tag{9}$$

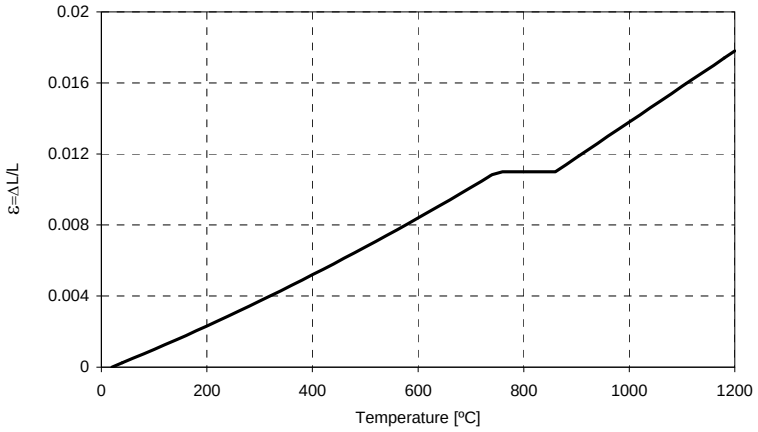

Fig. 8- Thermal elongation of steel as a function of temperature.

The figure 8 represents the steel capacity to increase its length when submitted to temperature action. After a first pending, this material property stabilize its value, due to the austenithique transformation that will depends on the heating rate. Above the 900[ºC] the steel element will continue to grow its length proportionally to the increase of temperature, but the mechanical steel resistance has short influence on the stability of structural elements.

3.1.2.- Modulus of Elasticity

In the linear elastic range, the elastic modulus will change due to the temperature increasing as it can be seen in the figure 9.

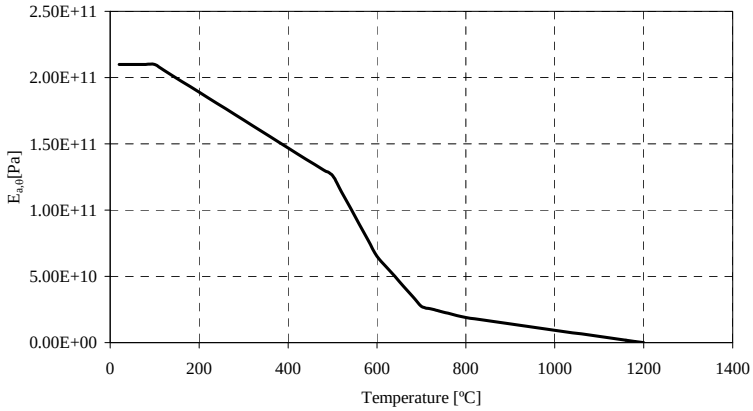

Fig. 9- Elastic modulus as a function of temperature.

This variation is the result of a tabulated relationship between the value of the modulus of elasticity at elevated temperature and the reference value at room temperature, equations 10.

$$k_{E,\theta} = \frac{E_{a,\theta}}{E_a} \tag{10}$$

Other authors present analytical expression for this property as a result of several numerical tests that represent the property behavior.

3.1.3.- Yield strength

Due to the non linear steel material behavior, a specific value of strain is defined to represent this value. At normal temperature is usual to use 0.2% of the material deformation, while for elevated temperatures is usual to fix 0.5% of the same measured entity.

After several experimental and numerical campaign, Franssen [3] propose several analytical expressions for represent the behavior of this property. In Eurocode the property variation is presented from tabulated results, as a coefficient that references the material property value to that at room temperature, expression 11.

$$k_{y,\theta} = \frac{f_{y,\theta}}{f_y} \tag{11}$$

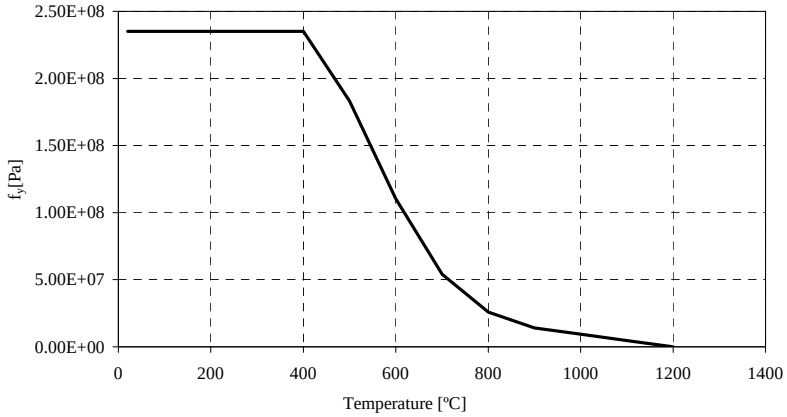

Fig.10.- Yield strength variation with temperature.

This material property has a crucial influence in buckling resistance of the structural element that it will be presented here. The abrupt decreasing of the yield strength after 400[ºC] is one of several factors that influences the diminution of buckling resistance.

Grain refinement is the most important strengthening mechanism in structural steels because it is the only method of strengthening which is accompanied by an increase in resistance to brittle fracture. The grain boundaries are barriers to dislocation motion. Consequently as the grain size is decreased, the number of barriers increases and this is reflected in increased yield strength.

3.2- Thermal properties.

The empiric Fourier equation used to study the behavior of the thermal conduction on solid bodies, uses three thermal material properties in its formula. The specific mass and the specific heat are used in the non steady state conditions and the conductivity is used in both cases.

The specific mass will be considered independent of the temperature evaluation with the value of 7850 [kg/m^3].

3.2.1- Specific heat

The capacity to store energy or the energy amount to heat the steel material defines this property. The temperature increase during a fire situation causes drastic changing in this property, because this material consumes a lot of energy in metallurgic transformation, during the 600 to 800 [ºC].

The variation of the specific heat is illustrated in the figure 11 and for simple calculation models this property may be considered constant to the value of 600[J/kgK].

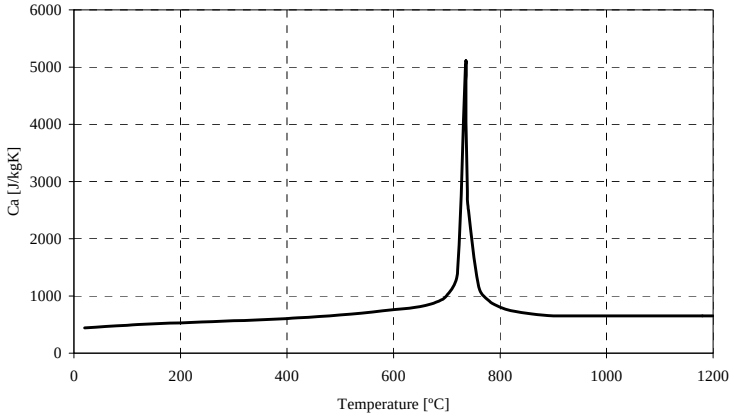

Fig. 11- Specific heat of steel as a function of temperature.

The analytical expression presented in [1] are the following:

$$
\begin{aligned}
C_a &= 425 + 7.73\times10^{-1}(\theta_a) - 1.69\times10^{-3}(\theta_a)^2 + 2.22\times10^{-6}(\theta_a)^3; \quad 20 < \theta_a \le 600[^{o}\mathrm{C}] \\
C_a &= 666 - \left[\frac{13000}{\theta_a - 738}\right]; \quad 600 < \theta_a \le 735[^{o}\mathrm{C}] \\
C_a &= 545 + \left[\frac{17820}{\theta_a - 731}\right]; \quad 735 < \theta_a \le 900[^{o}\mathrm{C}] \\
C_a &= 650; \quad 900 < \theta_a \le 1200[^{o}\mathrm{C}]
\end{aligned}
\tag{12}
$$

3.2.2- Thermal conductivity

The conductivity of steel material is high but it decreases in the inverse sense of the increasing temperature, during a fire situation, as it is presented in the figure 12.

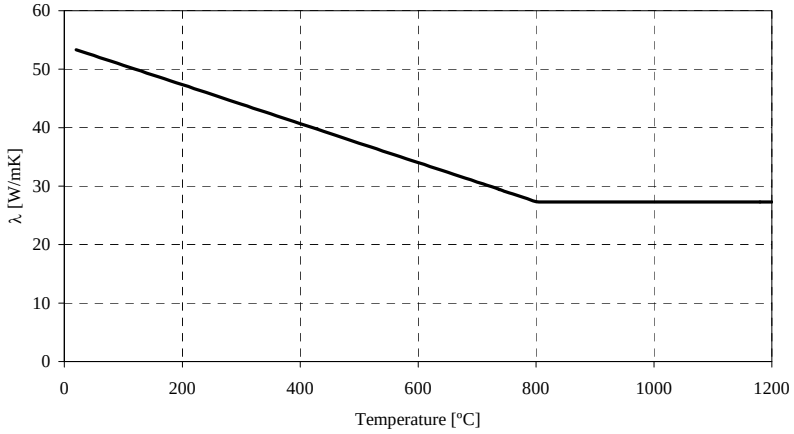

Fig.12- Thermal conductivity of steel as a function of temperature.

The analytical formula to represent the bi linear behavior of this material property can be approximated by the next set of equations, where it can be verified by the monotonous decrease from 53.3 to 27.3 [ºC] followed by a constant value over 800[ºC].

$$\lambda_a = 54 - 3.33\left(\frac{\theta_a}{100}\right);\quad 20 < \theta_a \le 800[^{o}\mathrm{C}]$$
$$\lambda_a = 27.3;\quad 800 < \theta_a \le 1200[^{o}\mathrm{C}] \tag{13}$$

For simple calculation models the thermal conductivity may be considered to be independent of temperature.

4-EXPERIMENTAL SETUP FOR MEASURE LATERAL TORSIONAL BUCKLING

As a result of the R&D project it was necessary to build a support structure and all the necessary equipment for loading and measuring the necessary parameter during this phenomenon (figure 1). A multifunction structure with 8 x 1.2 [m] was used to fixe the beam and apply the forces. The Electro hydraulic power system with two hydraulic jacks with 60 [ton] each gave the possibility to simulate the mechanical action on the beams and the electric ceramic mat were used to simulate a fire condition, rising and controlling the temperature in the way we intended to be.

The initial conditions of the steel beams were measured, specially, the residual stresses, the geometric imperfections and the cross section geometry was dimensionally controlled. Most of this information was a result of the steel process fabrication and of the packing process during transportation and storing.

The rolling process reduces the thickness of the section and changes its shape. As a process result and after rolling phase, the steel will gradually cools. The cross sections will have a non uniform temperature distribution and the root of the web maintains its bigger temperature for a long period than the other parts. This differential cooling leads to residual stresses that can influence the behavior of steel work under load.

The residual stresses in a single structural component or in a global structure are always present even without any service load. Fabrication processes like foundry, welding, machining, heat treatment and other factors, are the most common causes in this stress state. Other possible causes are those related to structural repair or modifications in their components. In same cases the stresses can be introduced in the structure by means of installation procedures, over load or other type of variable loads.

The effects of residual stresses in structural components may be positive or negative, depending on the magnitude, signal and their distribution relative to those induced by external loads. Several reported cases presents these residual states as the predominant factor for structural collapse.

4.1 Residual stresses measurement.

The magnitude and geometric distribution of the residual stresses may vary with the geometry of the cross section and with the straightening and cooling processes. The idealized distribution is expressed in the figure 13 and will be used to measure the residual state in four point of the beam.

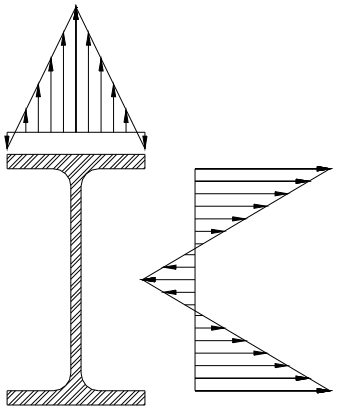

Fig.13- Residual stresses distribution over the cross section.

Some other authors present a parabolic distribution, taking into account the thermal phenomenon during the cooling process.

The measure of residual stresses in opaque elements can not be done by the traditional methods used in experimental stress analysis because the deformation sensors (extensometers, photoelastic materials, etc) are totally insensitive to the structural element history. For measuring the residual stresses with a strain gauge it will be necessary to free those storing stresses in some way that the sensor can detect a change in the state. This procedure presents a destructive characteristic in the passed, with the removing of successive surface layers of component material.

The present system setup for measuring the residual stresses is based on the drill hole method. The use of strain gages will be done but it will be necessary to introduce a mechanical interference in the system. The requirement of keeping the disturbance as small as possible is a positive factor in this method. The drill hole method as presented in the figure 14 requires a small drill hole of about 1.5 [mm]. This can be regarded as a non destructive technique.[11]

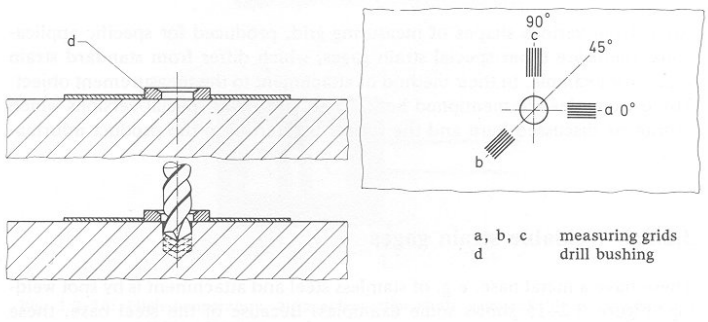

Fig.14- Drill – hole rosette.

With this type of rosette the strain gages respond with a deformation by means of relaxing the residual stresses, with the removing of the material. The residual initial stresses can be determined by the measured deformations and by the elasticity theory.

The residual stresses were measured in four points for each beam series, as it is shown in the figure 15.

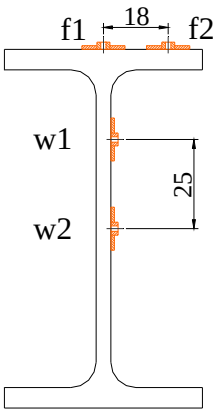

Fig.15- IPE100 cross section and drill - hole rosette positions.

The results on this four points are presented in table 1, but an average should be used for the input in either numerical and analytical calculations.

Specimen	Flange (f1) [MPa]	Flange (f2) [MPa]	Web (w1) [MPa]	Web (w2) [MPa]
P31	NM	8	NM	1
P23	NM	NM	NM	20
P34	45	NM	NM	NM
P33	41	15	NM	20
P44	NM	4	NM	38
P40	54	18	-22	26
P37	80	6	-12	20
P01	35	NM	-32	6
P21	46	7	-25	34
P11	50	31	-12	NM
Average	50	13	-21	21

Table1- Experimental results of residual stresses.

The residual stresses were measured over 40 places, which make possible to measure 10 different beams. Some of them were not take into account because the drilling tool crashes and the results (NM) could be dangerous to be stored. The process can be shown in the figure 16.

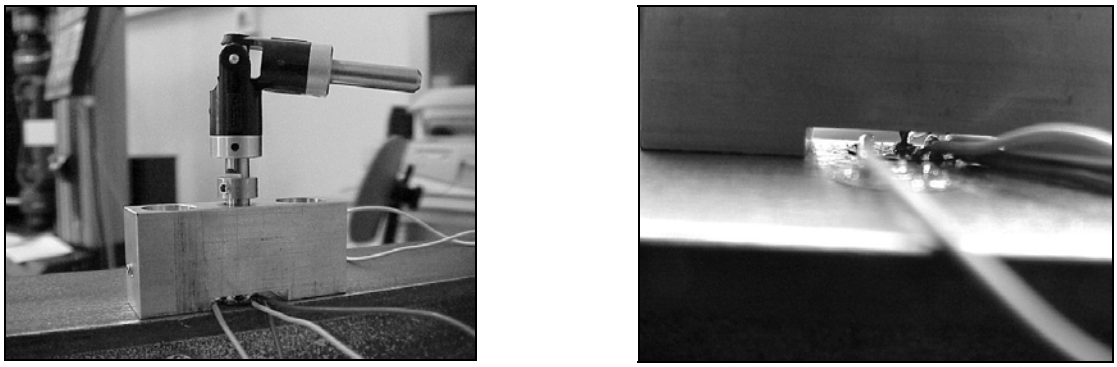

Fig.16– Residual Stress measurement – Hole drill method.

The set up for measuring presented in the Fig 16 represents the technique of hole drilling. It was also necessary to use the Spider 8 HBM system for acquisition data. This methodology is base on the relaxing stresses by means of a drilling hole. In the neighborhood of this a strain gage rosette is present and capable of measuring the difference between those states. The drilling operation should be careful and supported by a auto center block.

4.2 Measurement of geometric imperfection.

The beams presented different curvature caused by their own fabrication process, by the transportation or storing process. The procedure for measuring the geometric imperfection used a beam laser Helium Neon 30 mW – classe III b, as can be seen in the figure 17. This set of equipment use a magnetic support with a ruler that moves along the beam and measure the distance between the laser beam and the beam it self at discrete points. This values were recorded in five discrete points and used to approximate the shape of the imperfect beam.

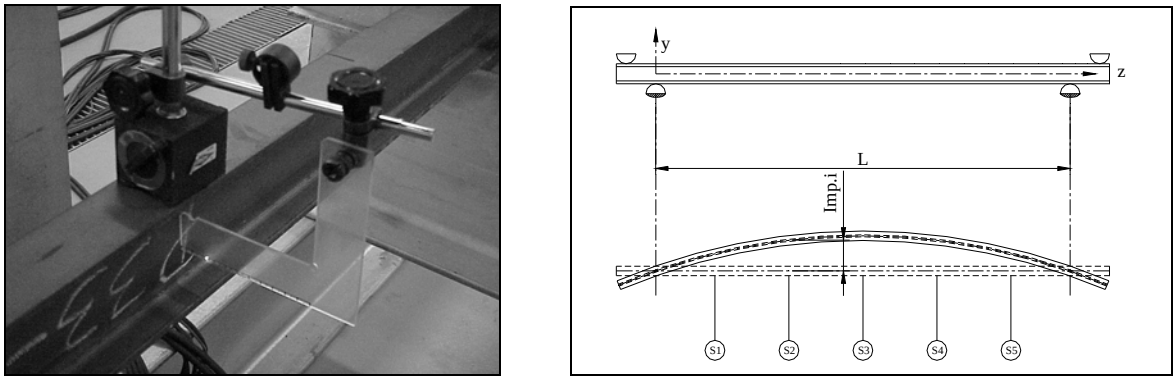

Fig.17- Geometric imperfection measuring setup.

The results of this measuring system can be done with a precision of 0.05 [mm], and make possible to measure the 120 lengths of tested beams.

For all measured geometric imperfection it an harmonic function was used to translate the non straight state of the beam as can be seen in the equation 16.

$$u(z) = \mu \,.\, Sin\left(\frac{\pi \times z}{L}\right) \tag{16}$$

where μ represents the maximum deviation amplitude to the laser beam for each measured beam. This function represents approximately the physical state of each of the tested beam, after treated the measured data. In table 2 is recorded the maximum amplitude of the measured values for each beam buckling length.

Tests at θ [ºC]	Beam 0.5 [m] buckling length	μ	Beam 1.5 [m] buckling length	μ	Beam 2.5 [m] buckling length	μ	Beam 3.5 [m] buckling length	μ	Beam 4.5 [m] buckling length	μ	Beam 5.5 [m] buckling length	μ	Beam 6.5 [m] buckling length	μ
20	P31	0.5	P33	1.0	P36	1.5	P01	3.0	P20	7.0	P22	3.0	P11	7.0
20	P31	0.5	P33	1.0	P35	1.5	P02	1.0	P17	5.0	P23	3.0	P17	7.0
20	P31	0.5	P33	3.0	P36	0.5	P07	3.0	P20	5.0	P27	3.0	P12	4.0
200	P31	0.5	P33	0.5	P38	1.0	P38	1.5	P23	2.5	-	NM	P19	3.0
200	P31	0.5	P34	1.0	P41	1.5	P38	3.0	P21	3.0	-	NM	P20	4.5
200	P04	0.5	P33	0.5	P39	1.5	P39	1.0	P30	2.5	-	NM	P14	4.0
300	P05	0.5	P33	0.5	P38	1.0	P41	3.5	P28	3.0	-	NM	P15	3.5
300	P02	0.5	P34	0.5	P37	1.0	P39	1.5	P24	3.5	-	NM	P?	4.0
300	P31	0.5	P34	1.0	P36	1.0	P40	1.0	P25	3.0	-	NM	P13	6.0
400	P07	0.5	P20	1.5	P40	0.5	P40	1.0	P15	2.5	P25	2.5	P18	7.5
400	P06	0.5	P09	1.0	P46	1.0	P37	2.0	P25	2.5	P08	3.0	P10	2.0
400	P31	0.5	P08	0.5	P44	2.0	P41	4.0	P26	2.0	P09	2.5	P02	3.5
500	P31	0.5	P43	1.0	P43	1.0	P06	1.0	P16	1.5	P29	3.0	P05	3.0
500	P31	0.5	P42	1.0	P42	1.0	P04	1.0	P14	2.5	P27	2.0	P07	6.0
500	P10	0.5	P44	1.0	P45	0.5	P05	2.0	P18	3.5	P26	2.0	P06	4.5
600	P03	0.5	P46	1.5	P42	1.5	P10	0.5	P13	4.0	P28	4.0	P01	8.0
600	P01	0.5	P45	0.5	P43	0.5	P09	1.5	P12	3.0	P30	1.0	P03	6.0
600	P31	0.5	P43	1.5	P46	1.0	P03	1.0	P	2.0	P22	2.0	P04	2.0

Table 2- List of geometric imperfections identification for test beams.

A set of 46 beams with 12 [m] each were cutted in the final necessary lengths and dimensionally inspected before the temperature variation from 20 [ºC] to the load temperature.

The beam cross sections has been inspected in five zones, as presented in figure 17 and it can be verified that the real dimensions are bigger than the tabulated technical data from Arbed.

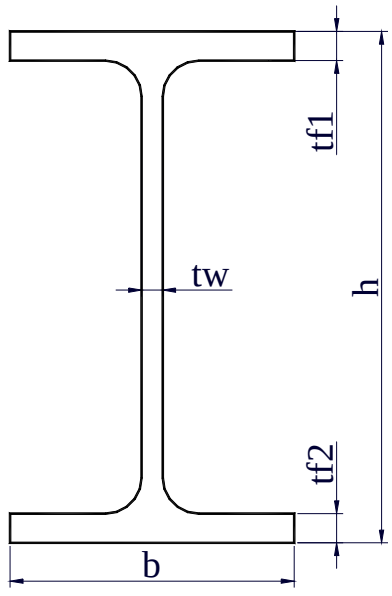

Tabulated Tech. data from Arbed	h [mm] 100	b [mm] 55	tf1 [mm] 5.7	tf2 [mm] 5.7	tw [mm] 4.1
Specimen	h	B	tf1	tf2	tw
P03	100.0	55.4	6.4	6.5	4.1
P04	100.3	55.7	6.2	6.4	4.2
P05	100.3	55.7	6.0	6.3	4.1
P06	100.7	55.8	6.1	6.5	4.2
P07	100.7	55.8	6.3	6.2	4.0
P08	100.4	55.5	6.0	6.7	4.0
P09	100.8	57.5	6.4	6.1	4.2
P10	100.9	56.0	6.1	6.6	4.1
P13	100.5	55.5	6.5	6.0	4.0
P14	100.4	55.4	6.3	6.4	3.9
P15	100.0	55.5	6.7	6.4	4.0
P19	100.5	55.4	6.3	6.4	3.9
P21	100.5	56.3	6.9	6.3	4.1
P24	101.0	55.6	6.0	6.1	4.2
P25	100.7	55.4	6.2	6.3	3.8
P26	100.4	55.4	6.5	6.7	4.0
P28	100.9	57.2	6.3	6.3	3.9
P29	100.3	55.3	6.3	6.1	4.3
P31	100.5	55.3	6.5	6.3	4.0
P33	100.4	57.0	6.4	6.1	4.1
P34	100.3	56.4	6.1	6.1	3.8
P36	100.3	55.9	6.0	6.4	3.9
P37	100.4	56.0	6.4	6.1	4.1
P38	100.4	56.0	6.9	6.9	4.2
P39	100.4	55.5	6.2	6.3	4.1
P40	100.6	56.1	6.4	6.1	4.0
P41	100.6	55.8	6.5	6.6	3.9
P42	100.5	55.9	6.2	6.5	3.9
P43	100.3	56.9	6.0	6.3	3.8
P44	100.6	56.8	6.7	6.5	4.2
P46	100.6	55.5	6.4	6.5	4.0
Avarege	100.5	55.9	6.3	6.4	4.0
Stand. Desv.	0.23	0.6	0.2	0.2	0.1

Fig. 17 – Points of inspection on beam cross section.

The real dimensions will be used to calculate the plastic modulus and all the necessary strength resistance parameters.

4.3 Mechanical strength characterization.

A set of 20 specimens were tested in the laboratory of the Polytechnic Institute of Bragança, using the 4485 Instron universal machine. The specimens were machined from the flanges and web parts of the IPE100 beams, and follow the Portuguese norm NP EN 10 002-1for mechanical strength characterization in terms of yield strength and elastic modulus. [12]

Fig.18– Universal machine during a strength test.

The tests were done at normal conditions and at a reference velocity of 2.5 [mm/s]. The result of 20 tests were treated and are presented in the table 3.

Beam	Location	Maximum load [kN]	Stress at maximum load [MPa]	Elasticity Modulus [MPa]	Yield Strength [MPa]
P31	web	55.410	412.031	209447	305.024
P31	web	54.090	402.216	202930	297.837
P31	web	54.630	406.231	324456	302.828
P31	web	55.650	413.816	156675	322.790
P20	web	56.910	432.447	257548	321.287
P24	web	57.720	435.952	220890	334.552
P30	web	58.820	445.606	232605	345.125
P30	web	58.010	440.805	182795	338.218
P25	web	57.610	440.443	294006	330.025
P21	web	57.660	443.538	166271	345.065
P26	web	56.750	419.438	262188	316.866
P31	flange	57.150	424.970	146026	325.984
P31	flange	54.090	402.216	202930	297.837
P31	flange	69.800	452.772	186776	315.000
P31	flange	60.480	449.732	229050	311.811
P31	flange	62.070	450.566	262974	312.377
P31	flange	63.170	453.026	217057	316.210
P31	flange	NM	NM	249754	315.000
P31	flange	NM	NM	146223	325.000
P31	flange	63.543	453.294	265968	320.000
Average		58.531	432.172	220828	320.000
S.D.		4.007	18.540	49019	14.000

Table 3.- Experimental results of strength tests.

The average results will be used for all the necessary calculations of the buckling cross section resistance.

4.4- Auxiliary equipment for experimental setup.

A multifunctional structure was built for the lateral torsional buckling experimental tests of I beam profiles under fire condition. This structure presents two movable supports and two other point loads with the same capabilities. This flexibility is necessary to leave the beam expands during the fire simulation, and to test different buckling lengths.

For fire simulation, a heating system with 70 [kVA] and all the necessary components for thermal energy generation were used. The temperature variation for rise and fall should be controlled, the heating elements should deliver the necessary power and provide the thermal insulation for best thermal efficiency.

Two different types of Electro ceramic mat resistance's with 1220 x 45 and 610 x 85 [mm] with the maximum electric power of 2.7 [kW] each were used for thermal delivery into steel I beams. This material is capable to support 1050 [ºC], although our experiments were done up to 600 [ºC] and at a heat rate of 800 [ºC/h]. The temperature distribution along the beam should be considered uniform although there is always a difference near the supports of the tested beams as it can be proved by the registration of the temperatures of the thermocouples K type used. Those sensors had been welded to the tested each tested beam in several discrete points .

The displacements of the three point controlling the cross sections movement were measured by means of displacement transducers as shown in the figure 19.

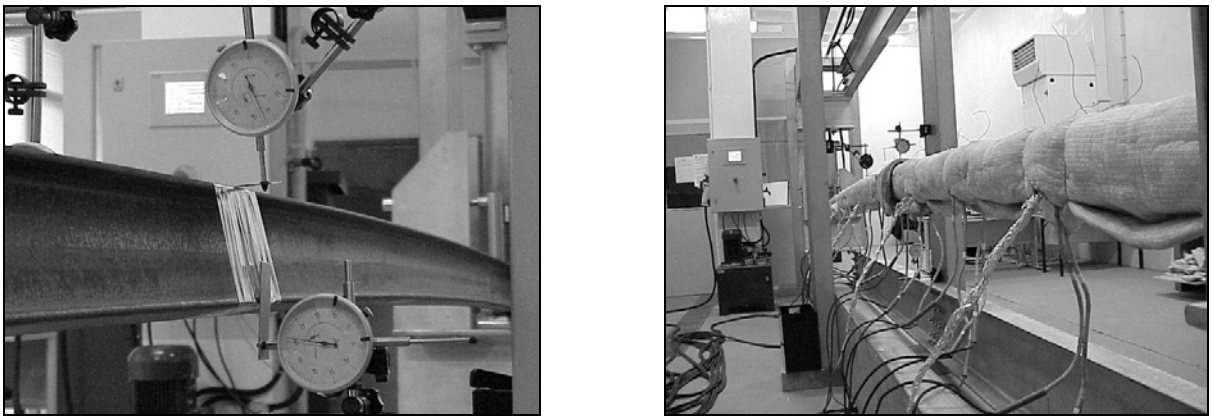

Fig.19- Displacement measuring system at room temperatures and at elevated temperatures.

In the case of elevated temperatures a metallic shield was used to make possible the contact of the displacement sensor with the tested heated beam.

4.5- Methodology of the experiments

The geometric imperfections were measured for each I beam in position to test and for those that would be submitted at elevated temperatures it was necessary to instrument thermally with the equipment described in the previous chapters.

During temperature rise the distance between the support and the point load was controlled and fixed after stability of temperature was achieved. After that, the mechanical load is applied and incremented up to the collapse load, as can be seen in the figure 20.

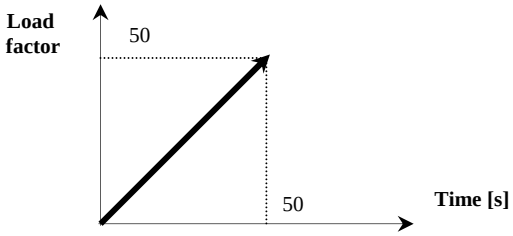

Fig. 20 – Load factor used for load increment.

All the collapse loads were recorded and transposed to critical moment to become possible a comparison to analytical formula, specially those from Eurocode.

5- THE NEW PROPOSAL FOR A SIMPLE MODEL IN LATERAL TORSIONAL BUCKLING.

According to the new proposal from Paulo Vila Real 1999 [16] and adopting for the lateral torsional buckling of beams the same proposal that Franssen used in 1995 [14] to represent the behavior of columns when submitted to fire conditions, the design value to buckling resistance in fire conditions should be calculated by the expression 16;

$$M_{b,fi,t,Rd} = \chi_{LT,fi} w_{pl,y} k_{y,\theta,com} f_y \frac{1}{\gamma_{M,fi}} \tag{16}$$

where $\chi_{LT,fi}$, $\phi_{LT,\theta,com}$ and $\overline{\lambda}_{LT,\theta,com}$ should be calculated as presented in Eurocode, as is the case of the reduction factor.

$$\chi_{LT,fi} = \frac{1}{\phi_{LT,\theta,com} + \sqrt{[\phi_{LT,\theta,com}]^2 - [\lambda_{LT,\theta,com}]^2}} \tag{17}$$

The overall buckling coefficient will be calculated as function of the imperfection factor. This imperfection factor α should now be a function of a severity factor β.

$$\phi_{LT,\theta,com} = \frac{1}{2}\left[1 + \alpha\overline{\lambda}_{LT,\theta,com} + (\overline{\lambda}_{LT,\theta,com})^2\right] \tag{18}$$

$$\overline{\lambda}_{LT,\theta,com} = \overline{\lambda}_{LT}\sqrt{\frac{k_{y,\theta,com}}{k_{E,\theta,com}}} \tag{19}$$

$$\alpha = \beta\varepsilon \tag{20}$$

This severity factor β should be chosen in order to ensure the appropriate safety level in the design of beams to lateral torsional buckling, and

$$\varepsilon = \sqrt{\frac{235}{f_y}} \tag{21}$$

where f_y represents the nominal yield strength of the material testing, $k_{y,\theta,com}$ the relative slenderness at room temperature, $\overline{\lambda}_{LT,\theta,com}$ the relative slenderness at elevated temperature, $w_{pl,y}$ represents the plastic moment of the cross section, $k_{y,\theta,com}$ the relative coefficient of the yield strength at the temperature $\theta_{a,com}$. The partial security factor in case of fire $\gamma_{M,fi}$ should be taken as 1.0.

Comparing equations (1) and (16) we can verify that with this new proposal we do not use the empirical constant 1.2 that is used as a correction factor in the proposal of the Eurocode 3. Equations (17) and (18) are exactly the same as those defined at room temperature in [13], except that the threshold limit of 0.20 for $\overline{\lambda}_{LT}$ does not appear in equation (18). This fact changes the shape of the buckling curve, beginning at $\chi_{TL} = 1.0$ for $\overline{\lambda}_{LT}$ but decreasing even for very low slenderness, instead of having a horizontal plateau up to $\overline{\lambda}_{LT} = 0.4$.

The lateral-torsional buckling curve varies with the yield strength due to the parameter ε that appears in the imperfection factor.

5.1. Experimental results

A set of 120 experimental results were done in Portugal. The beams in test were geometrically measured and its state of residual stresses also determined. The cross section geometry was averaged form a set of specimens and it could be verified that they didn't correspond exactly to the dimensions presented by the manufacture tabulated technical data.

The mechanical properties were considered from 20 measures on the specimens.

All beams were heated at a rate of 800[ºC/h] and the exposure to the experimental temperature $\theta_{a,com}$ was near the same, varying from 30[min] to 60[min] approximately.

The self weight from the ceramic mat, beam, and insulation material was considered to represent the relative buckling moment.

The results of each buckling moment were recorded and graphically presented in the terms of force against vertical displacement (DV), lateral top (DLC) and lateral bottom (DLB), with the system presented in the figure 21.

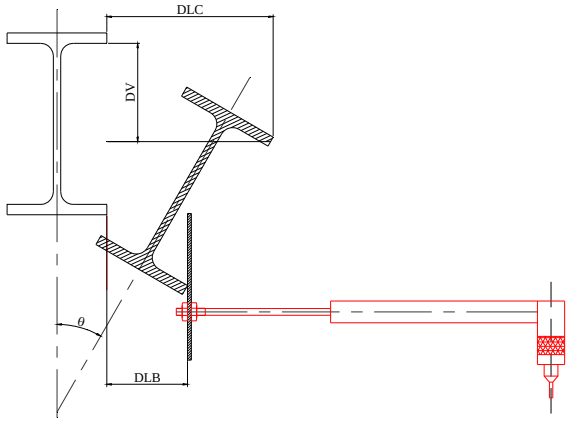

Fig. 21 – Displacement device for measuring displacement.

In figure 22 a resume of the tested beams set is presented for the extremes conditions of thermal load conditions, ie, at normal temperature and 600 [ºC] and for the extremes tested buckling lengths, ie, for 0.5 [m] and 6.5[m].

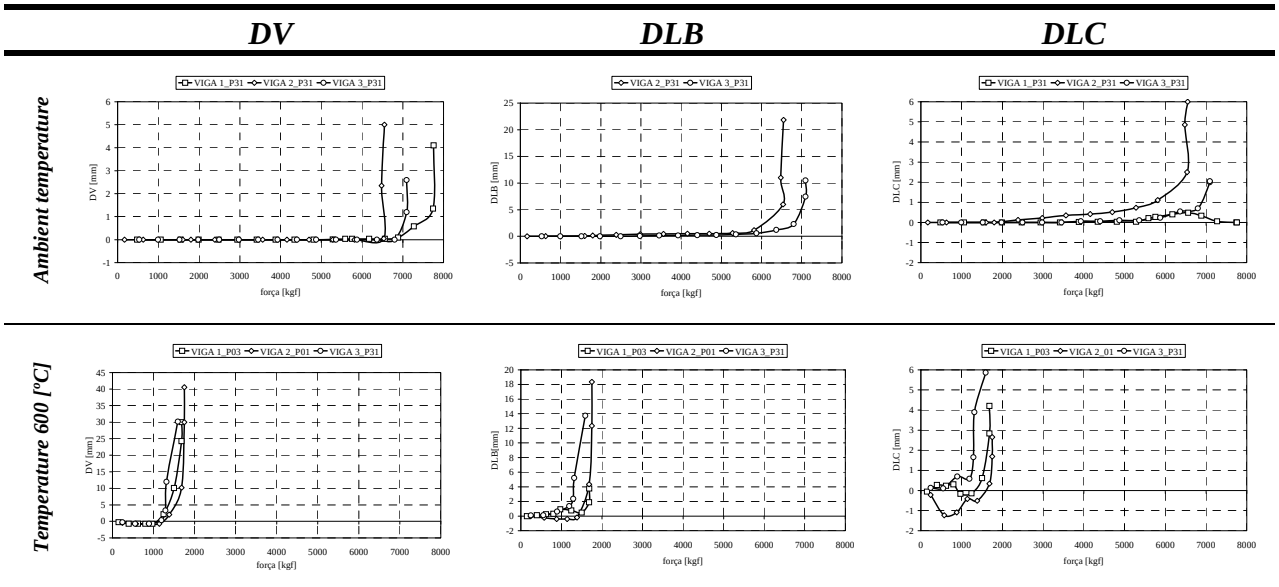

Fig. 22 – Mid span displacements for 0.5 [m] buckling length.

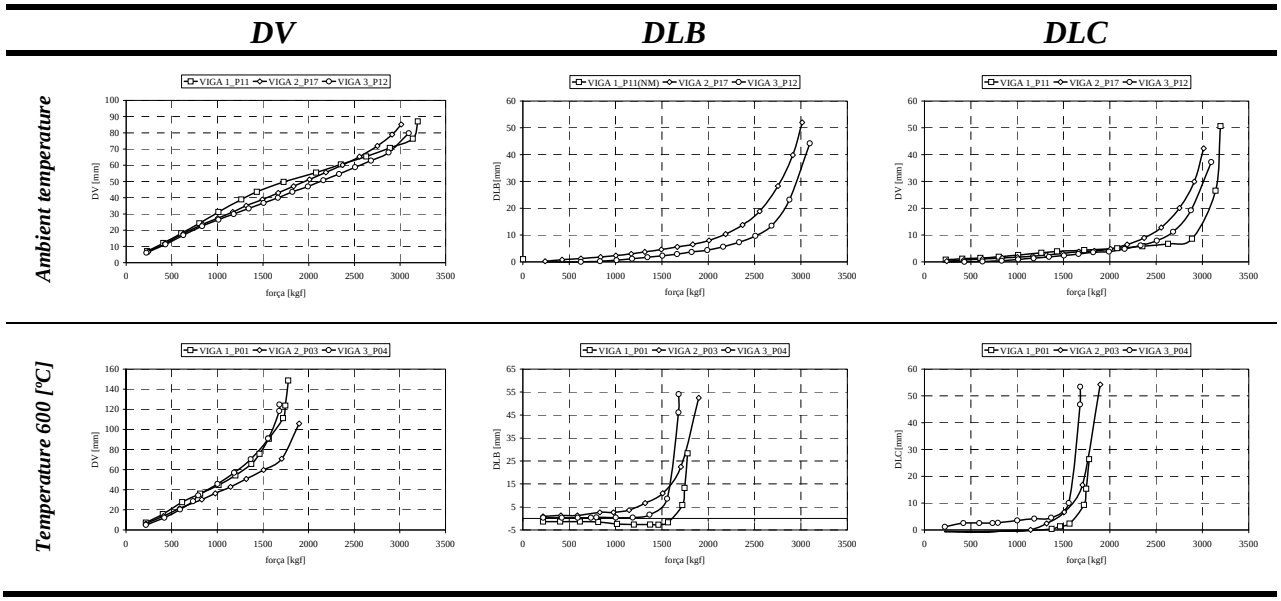

Fig. 23 – Mid span displacements for 6.5 [m] buckling length.

The last value of each experiment was considered to be the critical moment. As can be seen the buckling resistance decrease with the increase of temperature while the maximum displacement increases with the temperature at the collapse load.

The buckling resistance moment in terms of percentage of the cross section moment resistance can be represented against the dimensional slenderness at failure temperature. The result of all the tested buckled beams is presented in figure 24. Adopting the same value for the severity factor $\beta = 0.65$ that Paulo Vila Real used in its proposal, it can be verified that the results are in safe position except those for 0.5[m] of buckling length.

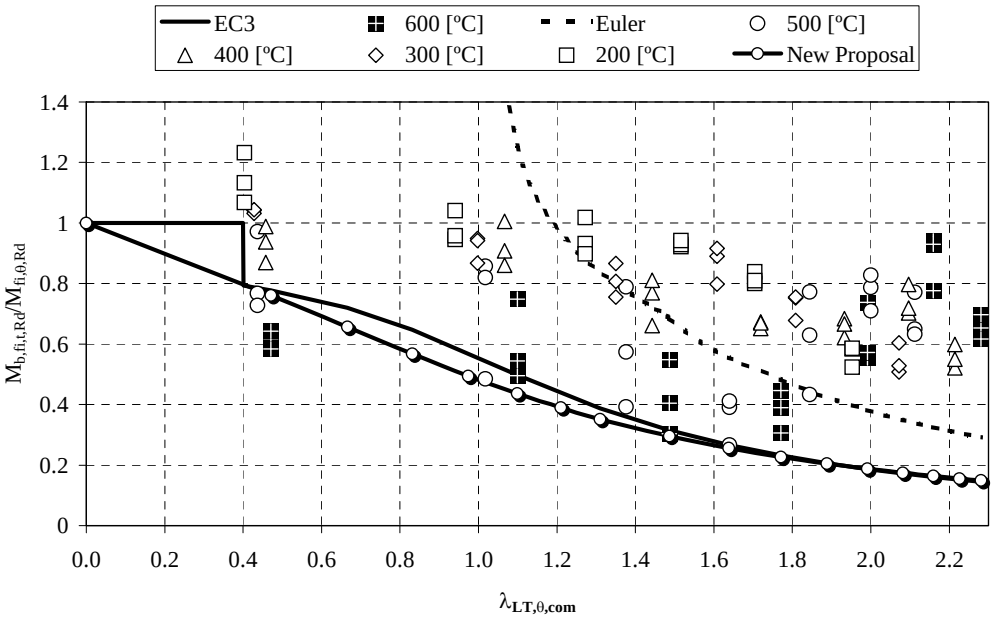

Fig. 24- Beam design curves at elevated temperatures.

6- CONCLUSIONS

The experimental results were done during several days, and the results could be influenced by a lot of parameters. First the temperature should or intended to be uniform, but in reality it does not occur, since the 4 temperature control unit only read the values in each thermocouple and action in conformity on rising and cooling of that region. Despite the beam insulation, this fact may influence the material properties and by consequence the results.

The time that each beam was exposed to fire was almost constant but those differences may be important for the creep situation.

The physical fact that Young's modulus decreases faster than the yield strength when the temperature increases, plus the fact that the stress-strain relationship at elevated temperature is not the same as at room temperature, produce a modification of the lateral-torsional buckling curve at elevated temperature. The horizontal plateau valid at 20 °C up to a non-dimensional slenderness of 0.4 may vanishes in the case of elevated temperatures like in the new proposal.

The simple models based on the lateral-torsional buckling curve that is valid at room temperature lead to a safety level that depends on the slenderness of the beam, even being unsafe for intermediate length beams. It has been possible to validate the new proposal of a lateral-torsional buckling curve for hot-rolled I-sections beams submitted to fire [16], based on the proposal suggested earlier [14] for axially-loaded hot-rolled H-sections submitted to fire.

The beam design curve based on the reduction factor for lateral-torsional buckling in fire design situation depends on the steel grade, which is not the case in the Eurocode 3, Part 1-2.

The severity factor β of the proposed simple calculation model has been established analyzing only the behavior of the IPE 100 profile. Further experimental results should be obtained to validate the value of the severity factor.

7- ACKNOWLEDGEMENTS

This work is a result of the National Portuguese Project of R&D that was financed by the Portuguese Foundation for Science and Technology (MCT/FCT) with the participation of the University of Aveiro and the Polytechnic of Bragança (Portugal).

The authors acknowledge the contribution of the enterprise J. Soares Correia, by the 500 [m] of IPE 100 beams that were tested in Bragança and the scientific support of the LOME (optics and experimental mechanical laboratory) of the University of Porto.

8- REFERENCES

[1]- ECS ENV 1993-1-2; Eurocode 3 – Design of steel structures – Part 1-2: General rules – Stuctural fire design"; 1995.

[2]- Trahair N.S. ; "Flexural Torsional Buckling of structures; E&FN SPON Chapman & Hall; London; 1993.

[3]- Franssen, J.M.; "Etude du comportment au feu des strutures mixtes acier béton, Thèse de doctorat; Collection de la F.S.A. ; Nº111; Univ. de Liège.

[4]- Rubert ª; Schumann P.; "Temperaturabhangige Werkstoffeigenshaften von baustahl bei Brandbeanspruchug"; Stahlbau; Verlag Wilh. Ernst & Sohn; Berlin; 54; Heft 3; 81-86; 1985.

[5]- ECS ENV 1993-1-1; "Eurocode 3: Design of steel structures – Part1.1: General rules and rules for buildings";1992

[6]- Stirland C.; "Steel properties at elevated temperaturares for use in fire engineering calculations";.Document ISSO/TC92/WG15/nº14; 1980.

[7]- RILEM; Y;"Proprieties of materials at high temperatures. Steel";. Anderberg éd.;Lund Inst. Of Tecnh.; 1993.

[8]- Ruge J., Winkelmann O. “Deformation behaviour of reinforcing and structural steel at high temperatures”; Sonderforschungsbereich 148, Brandverhalten von Bauteilen; Arbeitsbericht 1978; Part II; Braunschweig; 1980.
[9]- Skinner D.H; “Determination of high temperature properties of steel”; BHP Technical Bulletin; vol. 16; Melbourne Research Laboratories; 1972.
[10]- Skinner D.H “Behavior of steel during fires”; Melbourne Research Laboratories; 1972.
[11]- Hoffman Karl; “ An introduction to measurements using strain gages”; HBM publisher; Germany; 1989.
[12]- NP EN 10 002-1; CT12, Materiais metálicos:; “Ensaio de tracção. Parte 1: Método de ensaio”; Insituto Português da Qualidade; 1990.
[13]- Paulo M. M. Vila Real, Jean-Marc Franssen (1999) – “Lateral buckling of steel I beams at room temperature - Comparison between the EUROCODE 3 and the SAFIR code considering or not the residual stresses”, internal report No. 99/01 , Institute of Civil Engineering – Service Ponts et Charpents – of the University of Liege.
[14]- Jean-Marc Franssen, Jean-Baptiste Schleich & Louis-Guy Cajot, “A Simple Model for Fire Resistance of Axially-loaded Members According to Eurocode 3”, Journal Construct. Steel Research, Vol. 35, pp. 49-69, 1995.
[15]- Jean-Marc Franssen, Jean-Baptiste Schleich, Louis-Guy Cajot & Wenceslao Azpiazu “A Simple Model for Fire Resistance of Axially-loaded Members – Comparison with Experimental Results”, Journal Construct. Steel Research, Vol. 37, pp. 175-204, 1996.
[16]- Paulo M. M. Vila Real, Jean-Marc Franssen (1999) – “Lateral buckling of steel I beams at room temperature - Comparison between the EUROCODE 3 and the SAFIR code”, internal report No. 99/02 , Institute of Civil Engineering – Service Ponts et Charpents – of the University of Liege.